The United Nations University

GEOTHERMAL TRAINING PROGRAMME
Orkustofnun, Grensásvegur 9,
IS-108 Reykjavík, Iceland

Reports 1999
Number 7

GEOCHEMICAL INTERPRETATION OF THERMAL FLUID DISCHARGE FROM WELLS AND SPRINGS IN BERLÍN GEOTHERMAL FIELD, EL SALVADOR

María Inés Magaña Burgos
Comisión Ejecutiva Hidroeléctrica del Río Lempa (CEL)[1],
Gerencia de Recursos Geotérmicos,
Km 11½ Carretera al Puerto de la Libertad,
Santa Tecla, La Libertad,
EL SALVADOR, C.A.

ABSTRACT

The Berlín geothermal field is located in a tectonically very active area due to the subduction of the Cocos plate under the Caribbean plate. The chemical composition of waters in the study area is governed by water rock interaction. In this study, the Cl-SO_4-HCO_3 and Na-K-Mg triangular diagrams and stable isotopes were used to classify the geothermal and cold spring waters and to study some processes in the geothermal system. The geothermal waters are sodium chloride type with a high content of boron and lithium, indicating reactions with basic and acidic volcanic rocks. The cold spring waters are bicarbonate waters and the hot spring waters chloride waters.

The calculated quartz and chalcedony geothermometer values for the geothermal well waters indicate reservoir temperatures of 236-264˚C, lower than values for cation geothermometers, probably due to the fast reaction rate of silica at high temperature. The Na-K-Ca and N-K geothermometers give mostly higher values for the wells, or 262-304˚C. The gas geothermometers applied indicate temperatures of 232-295˚C. However, the calculation of mineral saturation indices for the geothermal waters shows fluid from all the wells to be close to equilibrium at 245˚C, and some degree of supersaturation with amorphous silica, chalcedony and quartz.

Two types of mixing models have been applied to evaluate the possible temperature of the hot water component in the geothermal springs, the chloride-enthalpy model and the silica-enthalpy model. These indicate subsurface temperatures of 174-216˚C. The chloride-enthalpy model was applied to determine some processes occurring in the field such as mixing, boiling and dilution. According to isotope results for wells TR-2 and TR-9, the El Hoyón fumarole (345˚C), located in the south-southwestern part of the field, could have fluid of the same origin. The steam from the Zapotillo and Tronadorcito fumaroles (276 and 339˚C, respectively) is probably of the same origin as the fluid from wells drilled in the southwestern part of the field after 1990.

[1] *Now: Geotermica Salvadoreña S.A. (GESAL)*

1. INTRODUCTION

El Salvador is located on the southern coast of Central America, where the Cocos plate is subducting under the Caribbean plate, forming an east-west tectonic graben. The Quaternary volcanic chain lies on the southern margin of this graben. Six high-temperature geothermal fields (280-320°C) have been identified lying on the northern flanks of this volcanic chain.

The Berlín geothermal field is located 100 km east of San Salvador, the capital city, and is located in the northwestern part of the Tecapa-Berlín volcanic structure. The area is tectonically very active due to the subduction of the Cocos Plate. The field is associated with the Tecapa volcanic group and the Berlín Caldera, which is of Pleistocene age. Figures 1 and 2 show the location of the Berlín geothermal field.

Geothermal exploration in El Salvador began in the mid 1960's with an investigation carried out by the United Nations Development Programme (UNDP). During this stage, two shallow wells and well TR-1 were drilled, revealing a commercially exploitable geothermal reservoir at depth (Monterrosa, 1993). During 1978-1981 five additional wells (TR-2, 3, 4, 5 and 9) were drilled, confirming the existence of a reservoir with commercial potential.

From 1990 and onwards, with reestablished confidence of financial institutions, a renewed effort was put into developing large projects such as the first condensing geothermoelectric plant at Berlín. One 5 MW well head back pressure unit was installed early on, but lack of injection wells delayed further progress. Since 1996 CEL has been developing the Berlín project and in 1999, a new power plant, that will produce around 55 MWe at full capacity, went on-line. From reservoir studies the estimated total capacity of the field is 100-150 MWe. To date, 16 new wells have been drilled (located in the north and southwest part of the field) to provide the necessary steam for power plant operation. Results of reservoir studies suggest that the drilling field could be extended to 10 km^2, which is an increase of 4 km^2 from previous studies.

Due to these expanded plans for the geothermal field several geochemical and isotope studies were carried out by CEL to characterise the cold and geothermal groundwaters. This report contains the results of data interpretation on water and steam from production and re-injection wells from 1995 to 1999. The study area is presented in Figure 3.

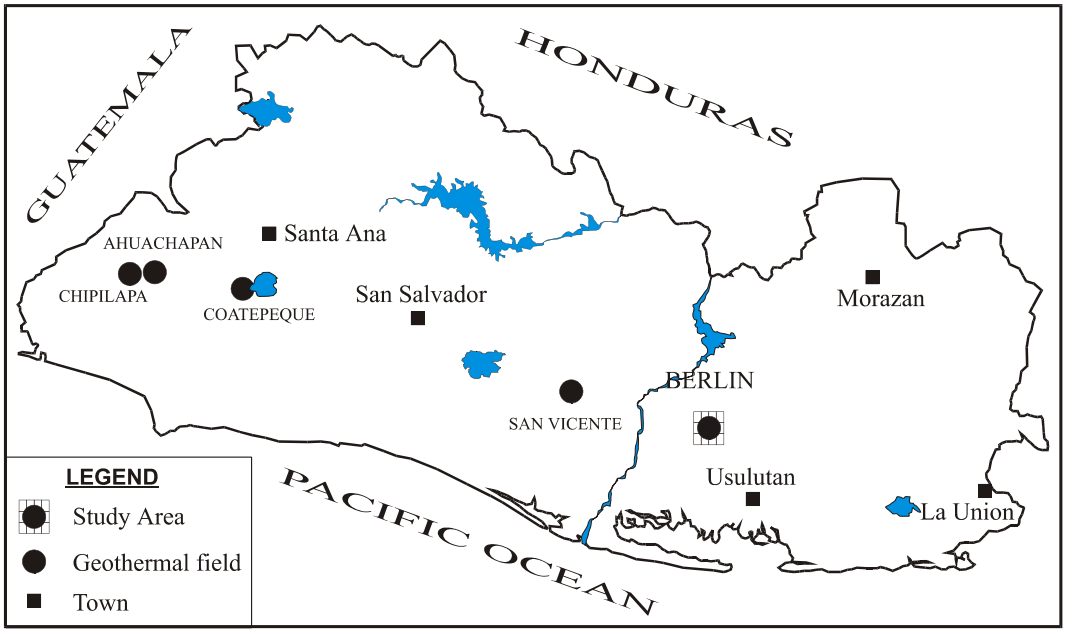

FIGURE 1: Locations of high-temperature geothermal areas in El Salvador

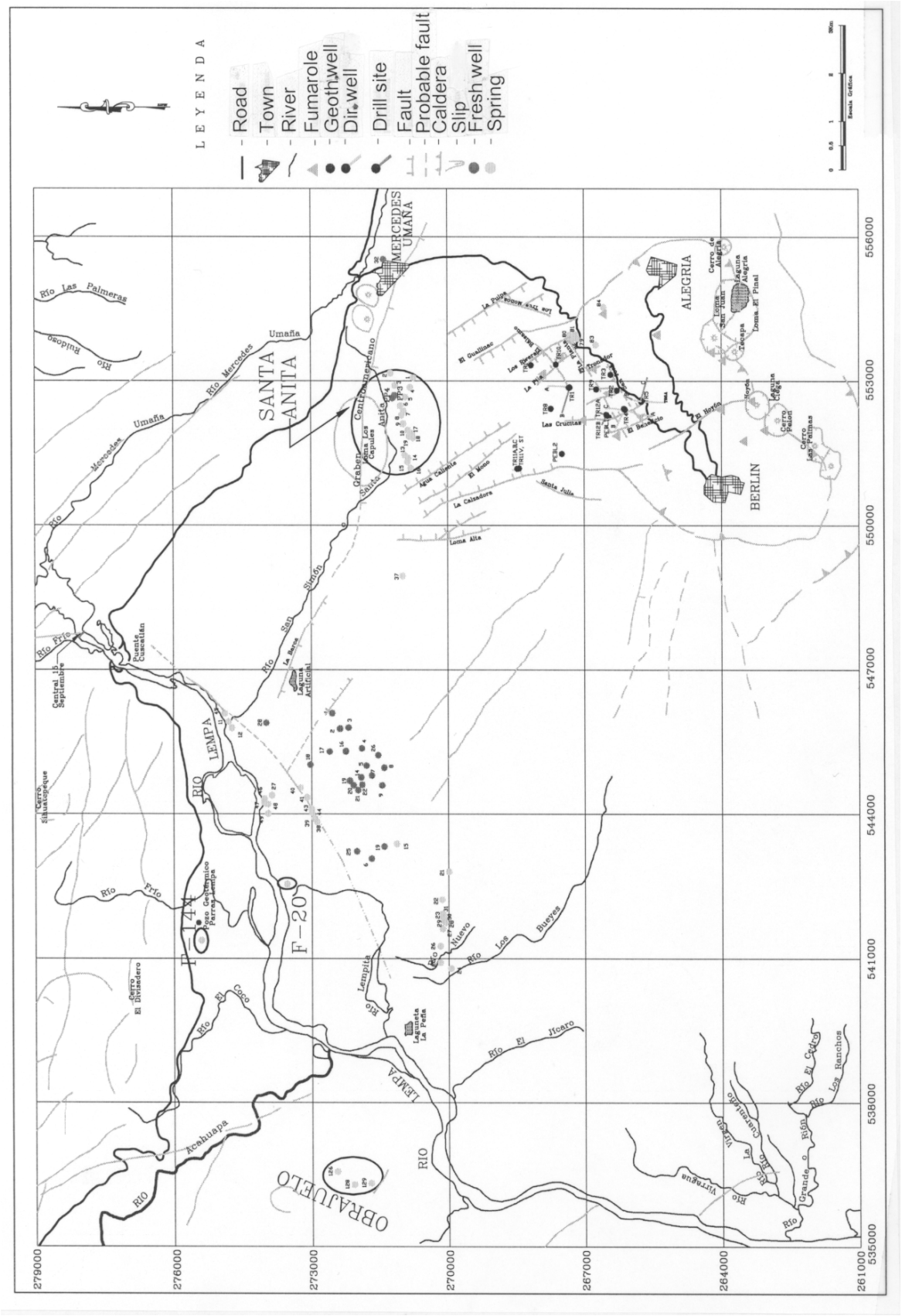

FIGURE 2: The Berlín geothermal field and surroundings

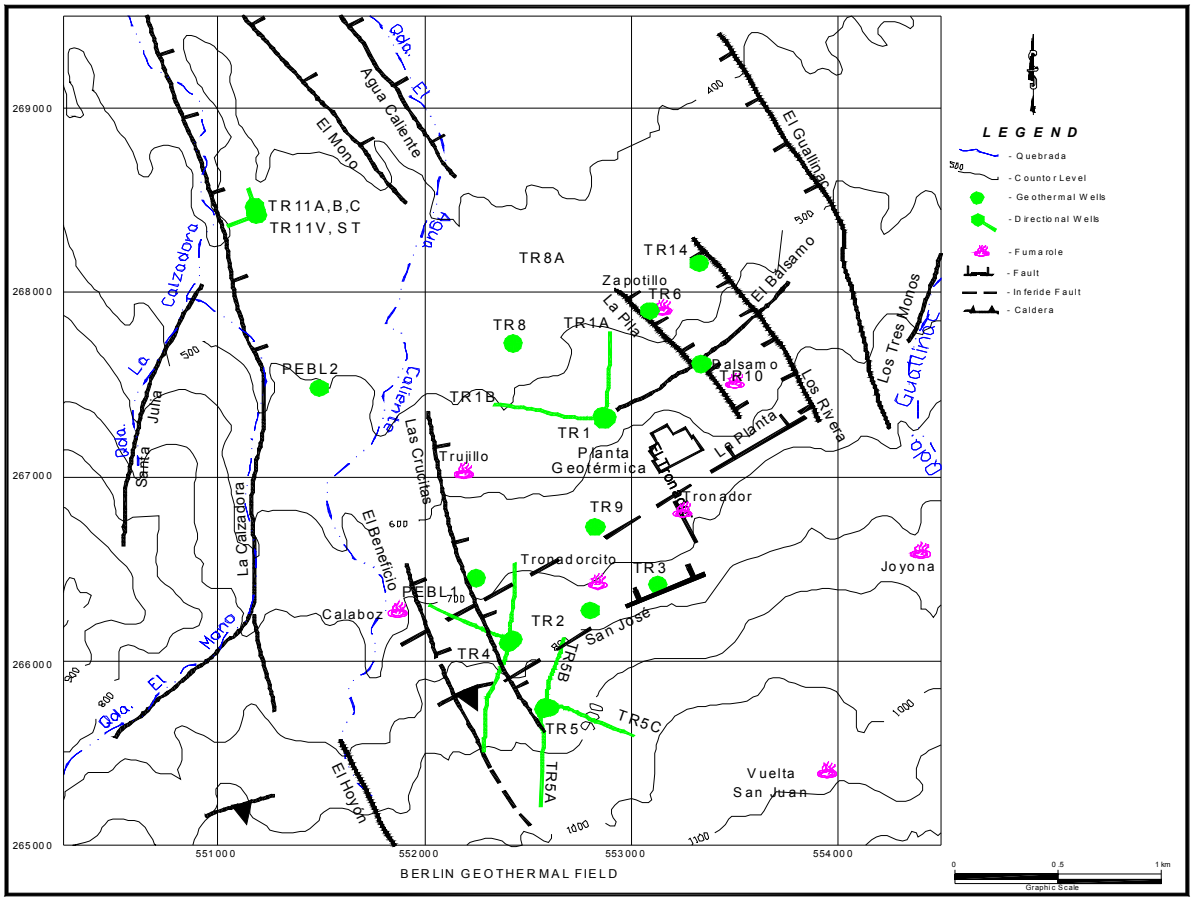

FIGURE 3: Location map of the Berlín geothermal field, showing tectonic features and wells

2. BERLÍN GEOTHERMAL FIELD

2.1 Geological and structural setting

The subduction of the Cocos plate under the Caribbean plate has formed a tectonic graben that runs E-W through El Salvador. The centre of the Berlín volcano appears to be where the regional northwest trending fault system intersects the southern margin of the E-W trending fault system forming the 5 km wide Berlín graben. The formation of the large basaltic andesite composite cone during the last 1-2 million years has twice been interrupted by explosive andesite eruptions forming black and grey ignimbrites. These eruptions were accompanied by a collapse of the upper part of the central cone, controlled partly by the previously existing northwest trending faults, and forming the outlines of the Berlín caldera (GENZL, 1995).

The geology of the field has been divided into annular faults formed by a caldera collapse, a regional fault system with a NE-SW orientation, perhaps related to a central graben, and a transverse fault with NNW-SSE orientation, maybe related to the caldera collapse. The NNW-SSE fault is younger and seems to be more active tectonically than the NE-SW faults. Several hot springs are aligned along these faults. A study of hydrothermal alteration in Berlín wells indicates that some fluid is moving along the older NE-SW faults, but geothermal fluids are also believed to be moving along the north-northwesterly directed faults.

The rocks of the Berlín area are of volcanic types with composition from basic to intermediate and intermediate-acid; some pyroclastic deposits are observed on the surface. The results of analysis of well cuttings show a succession of horizontal lava and tuff layers inside the lithological strata. These structures are believed to allow fluid movement; hence, relatively high horizontal permeability is expected in the region. The geothermal reservoir itself is mainly composed of highly fractured andesite rocks (Monterrosa, 1993).

2.2 Geochemical studies

Generally, the geothermal fluids discharged from the Berlín reservoir are classified as sodium-chloride type with pH between 5 and 8 and chloride content from 3000 to 7000 ppm. The gas/steam ratio is usually between 0.001 and 0.003 in steam from wells, but up to 0.085 in fumarole steam (mole/mole) and the salinity is between 7000 and 20000 ppm.

Results of chemical analysis allow the identification of three types of geothermal aquifers:

1. A low salinity (1600 ppm) shallow aquifer at depths between 200 and 300 m a.s.l.
2. Intermediate saline aquifers (6600 ppm) at sea level.
3. A deeper saline aquifer (8000-12000 ppm) at a depth of –800 to –1200 m a.s.l.

The chemical composition of fluids from fumaroles and hot springs indicates that the heat source is located beneath the Tecapa volcano and that the main flow of the geothermal fluid follows a NNW-SSE direction along faults, in good agreement with the resistivity survey carried out in the past years.

3. CHEMISTRY OF THE GEOTHERMAL FLUIDS

The composition of geothermal fluids depends on many factors, the most important being temperature dependent reactions between host rock and water. However, processes of mixing, boiling and cooling usually have a significant influence on the final composition of the geothermal fluids. The present study is based on 48 samples from cold and hot springs, and 29 samples from production and re-injection wells in the Berlín geothermal area (Figures 2 and 3). The chemical and isotopic composition of the samples is shown in Tables 1 and 2.

The samples from cold and hot springs and re-injection wells were collected in 1997. From 1995 to 1999, samples were collected from the wells both from weirbox and wellhead. The analysis was carried out in the chemical laboratory of Comisión Ejecutiva Hidroeléctrica del Río Lempa (CEL) in El Salvador, except some isotopic analyses (1995 and 1996) which were carried out in the isotope laboratory of the International Atomic Energy Agency (IAEA) in Vienna.

The temperatures of the cold and hot springs are between 37 and 98˚C and pH between 7 and 8. The chloride content of the samples collected ranges from 2 to 1142 ppm; most of the waters are HCO_3 type. A few (F-20, F-126, F-128, F-129, F-144B, F-145, F-146) are chloride type. Samples collected in the northwest part of the geothermal field do not have any relation to the Berlín geothermal system if isotope ratios are considered (Matus et al., 1999; Magaña, 1998). The chloride content of well discharge waters is between 2000 and 9000 ppm.

The isotope ratios for the production well fluids are found to be in the range -3.5‰ to -3.9‰ for $\delta^{18}O$ and -42‰ to -45‰ for $\delta^{2}H$. The isotopic composition of recently drilled well fluids changes with time, showing more depleted values of $\delta^{18}O$ (-4.92‰ to -6.62‰) and $\delta^{2}H$ (-44.63‰ to -50.88‰) to start with, but reaching normal values with time. The range of isotopic composition of re-injection well fluids is from -2.2‰ to -2.85‰ for $\delta^{18}O$ and from -38.7‰ to -44.35‰ for $\delta^{2}H$. These ratios show enrichment in heavy isotopes due to the flashing process during re-injection of wastewater (Matus, et al., 1999).

TABLE 1: Chemical and isotopic composition of Berlín geothermal well fluids (concentration in ppm, data from CEL, El Salvador)

Sample well	Na	K	Ca	Mg	Li	Cl	SO_4	HCO_3	SiO_2	B	pH	Enthalpy (kJ/kg)	S.P.** (bar-a)	$\delta^{18}O$ (‰)	$\delta^{2}H$ (‰)	Y (steam fraction)
TR-2/95	4170	970	23	0.161	17.1	7460	13.5	7.8	889	132	6	1311	3.3	-3.71	-48.6	0.34
TR-2/96	3185	684	28	0.085	12.7	5966	4.7	13.73	763	121	6.7	1378	12.2	-364	-44.8	0.29
TR-2/97	2123	490	40	0.1	8.3	3572	7		485	81	4.7	1348	8.9	-4	-45	0.3
TR-2/97	3600	803	94	0.07	15.2	6599	3.5	7.1	916	117	6.2	1348	10.7	-3.73	-44.6	0.29
TR-2/98	3623	812	76	0.107	14.6	6676	5.4	11.9	927	143	6.7	1419	10.2	-3.88	-43.9	0.33
TR-2/98	3850	890	28	0.06	13.8	6129	9	13.6	827	131	6.62	1419	11.8	-3.83	-45	0.31
TR-3/95	5323	1026	222	0.19		9407	17.6	42.7	1036	163		1438	3.2	-4.66	-49.9	0.4
TR-4A/98	1562	344	6.7	0.151	6.53	2527	44.2	65.4	771	61	7.8	1124	2.7	-5.25	-44.7	0.27
TR-4A/98	1634	364	12	0.943	7.52	2800	39.1	76	825	59	7.6	1124	1	-3.78	-42.5	0.29
TR-4B/98	1956	415	52	0.11	8.96	3372	44	54.6	856	76	7.5	1200	1	-4.92	-47	0.35
TR-4B/99	2536	562	70	0.25	8.79	4716	10.9	39.9	800	107	7.25	1066	2.2	-3.88	-43.2	0.25
TR-4B/99	2699	590	77	0.35	9.26	4769	11.9	43.7	828	116		1066	1	-3.78	-42.5	0.29
TR-4C/98	1590	358	7.1	3.3	5.18	2729	79.1		860	58	4.7	1144	1	-5.59	-47.1	0.32
TR-4C/99	2237	489	26	0.107	7.73	3812	5.8	10	723	99	6.5	1144	8.8	-4.12	-43.8	0.2
TR-5/95	2590	693	4.7	0.022	12.1	4697	9.4	18.1	942	119	6.7	1438	3.2	-4.66	-49.9	0.4
TR-5/96	2842	690	3.8	0.044	11.9	5051	10.9	13.4	1013	123	6.7	1438	7.9	-3.67	-42.4	0.35
TR-5A/98	1650	299	17	4.16	5.91	2642	93.6	16.7	801	66	5.5	1300	1	-5.41	-44.6	0.33
TR-5A/98	1455	265	13	4.04	5.18	2215	81.4	21	670	62	6	1300	3.5	-5.81	-48.8	0.39
TR-9/95	3765	817	119	0.107		6522	8.7	42.9	722	131	7.1	1232	4.4	-3.7	-45.1	0.29
TR-9/96	2510	577	56	0.1	11.9	4203	11.1	4.19	531	93	4.6	1347	8.78			
TR-9/97	3790	803	72	0.1	14.7	6507	0.5	27.23	726	124	6.9	1317	10.8	-3.62	-44.3	0.27
TR-9/98	3818	838	120	0.057	15.7	7127	7	25.51	853	150	7.8	1317	18.3	-3.37	-44.7	0.23
TR-9/98	3865	792	116	0.049	14.3	6385	9.4	26.34	711	138	6	1317	26.5	-3.45	-45	0.19
TR-1*	3760	858	96	0.1	15.7	6663	6.1	20.02	781	145				-2.45	-39.6	
TR-8*	3820	852	93	0.1	15.7	6698	6.6	19.77	803	144				-2.2	-38.7	
TR-10*	4780	1022	133	0.336	19.1	8364	22	18.36	604	162				-2.35	-40.2	
TR-14*	3845	848	94	0.1	15.8	6753	6	19.88	794	146				-2.38	-39.9	

*Reinjection wells **S.P.: Sampling pressure

TABLE 2: Chemical and isotopic composition of spring and domestic well waters in the Berlín area (concentrations in ppm)

Sample	Na	K	Ca	Mg	Li	Cl	SO_4	HCO_3	SiO_2	B	$\delta^{18}O$	$\delta^{2}H$
F-1	33.7	10.8	31.6	32.1	0.13	6.8	14.4	358	119	0.16	-6.9	-44.8
F-5	26.9	8.5	26.9	27.8	0	6.3	12.5	291	113	0.43	-6.9	-48.6
F-14	34.7	10.6	30.7	24.8	0	9.7	15	313	122	0.42	-6.9	-48.7
F-16	52.1	13.9	33.4	20.7	0	24.6	33.3	321	146	0.55	-6.7	-44
F-2	20	6.3	21.1	20.4	0	3.5	8.13	235	106	0.55	-6.7	-44.6
NSS	14.6	4.6	16.1	13.8	0	2.5	6.3	169	101	0	-6.8	-47.1
F-1	77.3	19.2	40.8	24.5	0.1	100	35.7	303	155	1.8	-6.6	-43.8
F-12	78.4	19.1	38.9	25.4	0.1	100	38.9	285	154	1.6	-6.6	-44
F-45	73.2	18.2	39.1	23.6	0.1	90	31.1	293	152	1.6	-6.7	-44.3
F-47	77.7	19.9	38.1	26.8	0.1	97.8	42.5	311	151	1.8	-6.7	-44.4
F-20*	287	9.83	81	1.8	0.25	356	266	102	118	5.5	-6.2	-41.7
F-49	68.3	18.9	40.4	28.9	0.1	79.8	52.8	322	147	1.32	-6.7	-45.5
F-41	50.7	17.5	24.8	29.3	0	28.5	34.1	330	129	0.4	-7.1	-45.8
F-43	30.1	8.5	24.2	17.2	0	8.2	42.4	209	109	0.3	-6.2	-40.3
F-26	18	7.9	32.4	19		8.8	9.5	229	92	0.1	-6.3	-41.8
F-44	30.8	9.1	32.2	20	0	9	38.7	235	107	0.4	-6.3	-41.2
F-22	17.2	6.2	21	15.6	0	4.3	3.7	192	92		-6.9	-48.5
F-30	16	6.1	21.8	16.2	0	7.5	4.3	196	91	0	-6.9	-45.6
F-29	15	5.6	25.9	14.1		4.7	3.5	185	96	0.11	-7	-46.7
F-25	17.7	7.8	39.2	20.3		12.1	15.4	228	95	0.11	-6.4	-43.9
F-15	44.4	11.7	45.6	23.7	0	19.1	26.6	313	131	0.37	-6.8	-46.5
F-24B	16.6	6.1	23.1	15.4		4	3.45	197	92	0.1	-6.8	-42.8
F-48	55.2	16.6	41.1	27.4		38.5	42.9	359	130	0.7	-6.6	-44.4
F-32	12.5	3.6	18.8	11.9		2.2	1.5	137	94	0.69	-6.8	-44.1
F-126*	700	22.1	133	0.6	0.33	1142	265	24.9	126	14	-5.5	-38.4
F-128*	700	22	133	0.7	0.33	1141	276	24.1	130	14.3	-5.4	-40.7
F-129*	703	22.4	133	0.9	0.33	1137	284	26.5	131	14.7	-5.4	-40.3
F-79	48.3	14.5	13.4	4.3	0	3.8	53.7	144	158	1.75	-6.9	-45.5
F-80	49.9	14.6	13.4	5		4.2	52	145	163	1.7	-6.9	-45.5
F-81	50.3	15	13.9	4.9		4.7	47.6	156	158	1.69	-6.9	-45.5
F-144*	337	13.4	73.1	0		495	241	52	173	6.9	-6.2	-42.1
F144B*	323	14.5	70.2	1.7		490	241	60	163	5.57	-6.2	-42.3
F-145*	327	13.1	58.2	0.13		446	227	60	172	7.13	-6.1	-41.6
F-146*	325	7.7	62.9	3.8		348	167	59	128	4.14	-6.2	-41.5
P-4	44.2	14.5	53.6	28.6	0	42	34.3	293	120	0.69	-6.7	-44.5
P-5	52.3	16.3	42.3	20.6		54	42.2	268	129	0.63	-6	-40
P-9	37.1	12.8	58.2	31.2	0	33.1	45.7	348	96	1.04	-5.8	-39
P-6	35.9	20.3	78.8	43.5		33.6	84.1	366	119	0.51	-6.3	-41.6
P-14	37	12.5	28.7	20.3	0	15.7	19.1	204	116	0.5	-6.4	-40.7
P-18	43.9	22.4	75	33	0	35.1	59.9	389	101	0.15	-6.8	-45.5
P-20	59	11.7	42.7	21.6	0	56.5	35.5	280	126	0.9	-6.7	-44.2
P-23	49.6	14.8	40.2	26.5	0	43.7	28.5	278	126	1	-6.6	-44
P-3	29	6.3	42.1	12.1	0	22.5	23.8	182	119	0.3	-6.6	-45.7
P-7	53.3	16.2	36.1	25.9	0	48.3	33.4	293	129	0.82	-7.3	-48.1
P-22	29	6.3	42.1	12.1	0	22.5	23.8	182	119	0.3	-6.6	-45.7
PHM	53.3	16.2	36.1	25.9	0	48.3	33.4	293	129	0.82	-7.3	-48.1
PA1	24.8	7.8	30.4	26		4.03	13.3	184	102	0.8	-7.4	-48.9
PA2	15.5	4.8	18.1	16.2		2.19	10.7	193	97	0.75	-7.3	-50.6

* Temperature > 60˚C

The ionic balance for the water analyses was calculated by the WATCH program (Arnórsson et al., 1983a; Bjarnason, 1994), and these results are in agreement with those obtained in CEL's laboratory. Ionic balance gives information regarding the quality of the analysis, at least for those ions that occur in the highest concentrations. Ionic balance for the analyses varies between –5 and 10% indicating that all the analyses are of acceptable quality.

3.1 Fluid classification

3.1.1 Stable isotope composition

Isotope variations occur in natural systems (gas-water-rock assemblages) as a result of natural processes. Techniques based on natural variations of these components are now common tools in geochemical surveys both during exploration and exploitation stages of the development of a geothermal area. Two opposing properties of isotope ratios are exploited; their tendency to vary due to fast, incomplete or unidirectional processes due to temperature changes, rock-water interactions, steam separation, dilution or mixing; and their ability to remain largely unaffected by physical and chemical processes during their move from source to sampling point, rendering them suitable as tracers.

The isotopic analyses of water samples from springs and wells will give us information on the origin of the fluid discharged, on its age, on possible underground mixing between different waters, on water-rock interaction, and on steam separation. The mean annual hydrogen and oxygen isotopic composition of precipitation in any area is related to the local mean annual temperature: the lower the temperature, the lower the content of heavy isotopes. The relationship between δD and $\delta^{18}O$ is given by:

$$\delta^2 H = 8\delta^{18}O + B \quad (1)$$

where the constant *B* (the deuterium excess) is, in most cases, close to 10. Its value, however, depends on climatic conditions, being low in a wet climate but higher in a dry climate. Figure 4 shows the relationship between δ^2H and $\delta^{18}O$ values of water from the study area.

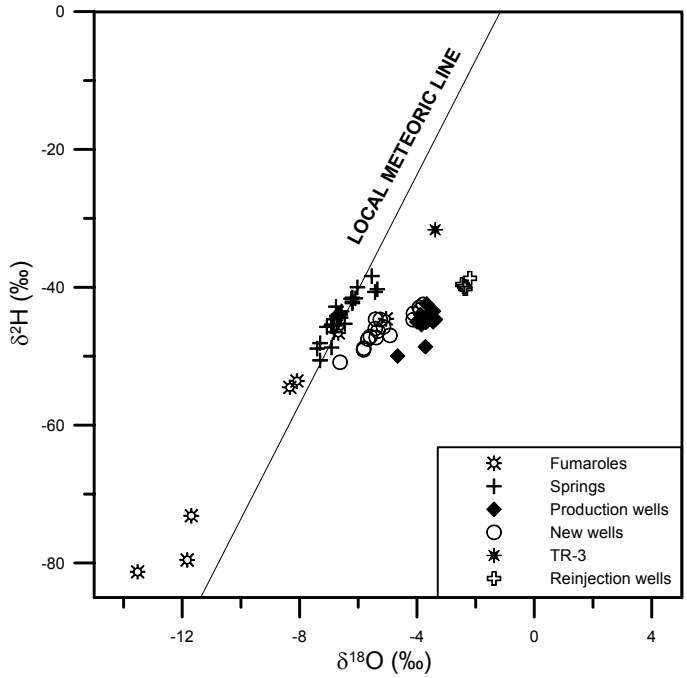

FIGURE 4: $\delta^{18}O$ vs. δ^2H for the Berlín waters

3.1.2 The Cl-SO_4-HCO_3 diagram

The interpretation of geothermal water chemistry is best carried out on the basis of an initial classification in terms of their major anions Cl, SO_4 and HCO_3. The position of a data point in such a triangular diagram (Giggenbach, 1991) is obtained by first obtaining the sum *S* of the concentrations of all three constituents involved. In the present case

$$S = C_{Cl} + C_{SO_4} + C_{CHO_3} \quad (2)$$

The next step consists of the evaluation of *%-Cl, %-SO_4* and *%-HCO_3* according to the following equations:

$$\%-Cl = 100\,C_{Cl}/S \;\; ; \qquad \%-SO_4 = 100\,C_{SO_4}/S \;\; ; \qquad \%-HCO_3 = 100\,C_{HCO_3}/S \quad (3)$$

The diagram also allows the immediate eyeball statistical evaluation of groupings and trends. It should, however, be kept in mind that any such three component plots tell only part of the story and that some apparent correlation may only be purely coincidental. The diagram may provide an initial indication of mixing or geographical groupings, with Cl waters forming a central core grading into HCO_3 waters towards the margins of a thermal area. The degree of separation between data points for high chloride and bicarbonate waters gives an idea of the relative degree of interaction of CO_2 charged fluids at lower temperatures, and the HCO_3 contents increasing with time and distance travelled underground. Figure 5 shows the results for the Berlín geothermal field samples.

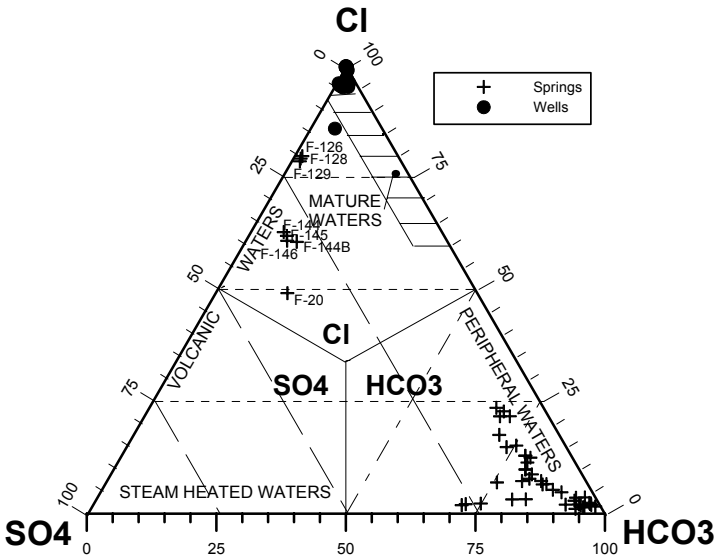

FIGURE 5: Cl-SO_4-HCO_3 diagram for the Berlín waters

3.1.3 The Cl-Li-B diagram

The alkali metal probably least affected by secondary processes is Li. It may, therefore, be used as a tracer for the initial, deep rock, dissolution process and as a reference to evaluate the possible origin of the other two important conservative constituents of thermal waters, Cl and B. Once added, Li remains largely in solution. It is, however, striking that both Cl and B are added to the Li containing solutions in proportions close to those in crustal rocks. At high temperatures Cl occurs largely as HCl, and B as H_3BO_3. Both are volatile and able to be mobilised by high-temperature steam. The position of a data point on the diagram is calculated by:

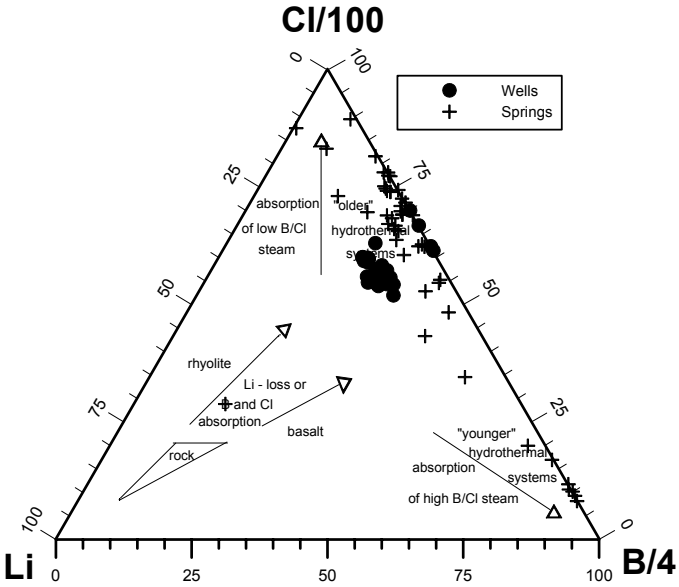

FIGURE 6: Cl-Li-B diagram for the Berlín waters

$$S = C_{Cl}/100 + C_{Li} + C_B/4 \quad (4)$$

$$\%-Cl = C_{Cl}/S \;\; ; \qquad \%-Li = 100\,C_{Li} \;\; ; \qquad \%-B = 25\,C_B/S \quad (5)$$

Figure 6 depicts the results for the Berlín area, the well water suggesting water from an ageing geothermal system, but spring waters a range from a young system to the same ageing one suggested by well water.

3.2 Geothermometers

Geothermometers are based on one or more constituents in geothermal fluids (either solutes or gases, and may include isotopes of elements) which are controlled in concentration or in certain proportions in a fluid, primarily by the temperature of the fluid and the surrounding rock. Many are based on particular chemical equilibrium reactions. Geothermometers can be applied to well or natural surface discharges to obtain approximate subsurface temperatures. It is also desirable that the temperature-dependent reactions are relatively fast at high temperatures but slow at low temperatures.

Since the 1960's various solute geothermometers have been developed to predict subsurface temperatures in geothermal systems, such as silica geothermometers (Fournier and Rowe, 1966; Fournier, 1977; Fournier and Potter, 1982; Arnórsson et al., 1983b), Na-K geothermometers (Truesdell, 1976; Fournier, 1979; Arnórsson et al., 1983b; Giggenbach, 1988). Na-K-Ca geothermometer (Fournier and Truesdell, 1973) and Na-K-Ca-Mg geothermometer (Fournier and Potter, 1979; Giggenbach, 1988).

These geothermometers all assume the attainment of chemical equilibria in geothermal systems. When applied to the same geothermal fluid, the different geothermometers frequently yield appreciably different subsurface temperatures due to a lack of equilibrium between the solution and hydrothermal minerals, or as a result of reactions, mixing or degassing during upflow. The solute geothermometers used in this report are discussed in the following sections.

3.2.1 Cation geothermometers

Cation geothermometers are widely used to calculate subsurface temperatures of water collected from hot springs and wells. There are many different geothermometers to choose from, and it is rare that they all give approximately the same result, especially when applied to hot spring waters. The theoretical basis for cation geothermometry is ion exchange reactions with temperature-dependent equilibrium constants. An example is the exchange of Na^+ and K^+ between co-existing alkali feldspars:

$$Na\,Al\,Si_3\,O_8 + K_+ \Rightarrow K\,Al\,Si_3\,O_8 + Na^+$$

Na-K-Mg triangular diagram. Giggenbach (1988) suggested that a triangular diagram with Na/1000, K/100 and $(Mg)^{1/2}$ at the apices can be used to classify waters as fully equilibrated with rock at given temperatures, partially equilibrated, and immature (dissolution of rock with little or no chemical equilibration). The full equilibrium curve is for reservoir water composition corrected for loss of steam owing to decompressional boiling. Uncorrected boiled waters will generally plot slightly above the full equilibrium line.

The Na-K-Mg triangular diagram provides an indication of the suitability of a given water for the application of ionic solute geoindicators. It is based on the temperature dependence of the full equilibrium assemblage of potassium and sodium minerals that are expected to form after isochemical recrystallization of average crustal rock under conditions of geothermal interest. The use of the triangular diagram is based on the temperature dependence of the three following reactions:

$$K\text{-}feldspar + Na^+ = Na\text{-}feldspar + K^+$$

$$0.8muscovite + 0.2clinochlore + 5.4silica + 2Na^+ = 2albite + 0.8K\text{-}feldspar + 1.6water + Mg^{2+}$$

$$0.8muscovite + 0.2clinochlore + 5.4silica + 2K^+ = 2albite + 2albite + 2.8K\text{-}feldspar + 1.6water + Mg^{2+}$$

The Na-K-Mg triangular diagram (Giggenbach, 1991) is obtained in an analogous manner to the two diagrams described above and the position of the data point on the diagram is calculated similarly using the following equations:

$$S = C_{Na}/1000 + C_K/100 + \sqrt{C_{Mg}} \quad (6)$$

$$\%\text{-}Na = C_{Na}/10S \;\; ; \quad \%\text{-}K = C_K/S \;\; ; \quad \%\text{-}Mg = 100\sqrt{Mg}/S \quad (7)$$

This diagram clarifies better the origin of the water. Corresponding waters were all shifted in the diagram, and the results for the study area are presented in Figure 7. It is also used to obtain Na/K and K/Mg geothermometer temperatures when the suitability of the water for such geoindicators has been established.

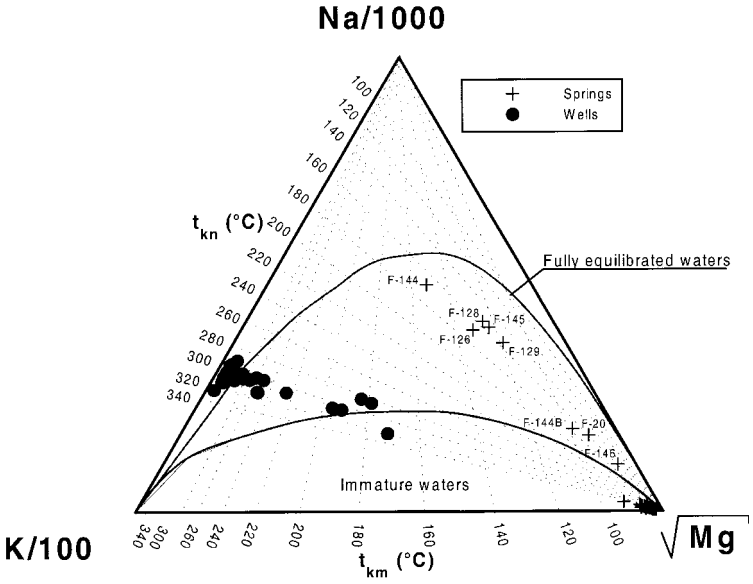

FIGURE 7: Giggenbach's Na-K-Mg triangular diagram for the Berlín waters

Many temperature functions have been presented for the Na-K geothermometers by various authors, but there is a large discrepancy between temperatures resulting from the different equations. The following formulae are used in this report (the concentration of Na and K are in mg/kg):

Na/K temperature (Fournier, 1979)

$$t(^\circ C) = \frac{1217}{1.483 + \log(Na/K)} - 273.15 \quad (8)$$

Na/K temperature (Giggenbach, 1988)

$$t(^\circ C) = \frac{1390}{1.75 + \log(Na/K)} - 273.15 \quad (9)$$

Na/K temperature (Truesdell, 1976)

$$t(^\circ C) = \frac{856}{0.857 + \log(Na/K)} - 273.15 \quad (10)$$

Na/K temperature (Arnórsson et al., 1983b)

$$t(^\circ C) = \frac{933}{0.993 + \log(Na/K)} - 273.15 \quad (11)$$

The K-Mg geothermometer (Giggenbach, 1988), based on the equilibrium between water and the mineral assemblage K-feldspar, K-mica and chlorite, is found to respond fast to changes in the physical environment and usually gives a relatively low temperature. This geothermometer is also reasonable for estimation of reservoir temperature (concentrations are in mg/kg):

$$t(^{\circ}C) = \frac{4410}{14.00 - \log(K/\sqrt{Mg})} - 273.15 \qquad (12)$$

The Na-K-Ca geothermometer (Fournier and Truesdell, 1973) takes into account a reaction involving the exchange of Na^+, K^+ and Ca^{++} with a mineral solid solution. This minimises but does not eliminate effects of disregarding the activity coefficients of solids. The geothermometer is entirely empirical and assumes a base exchange reaction at temperatures above 100˚C (concentrations are in mg/kg):

$$t(^{\circ}C) = \frac{1647}{\log(Na/K) + \beta[\log\sqrt{Ca}/Na + 2.06] + 2.47} - 273.15 \qquad (13)$$

$\beta = 4/3$ for $t < 100^{\circ}C$; $\beta = 1/3$ for $t > 100^{\circ}C$.

In natural systems, however, many different cations generally exist in solid solution within certain types of silicates, such as Na and Ca in plagioclase and Na, Ca, Mg, K, and Li in smectites.

3.2.2 Silica (quartz) geothermometer

The use of dissolved silica as a geothermometer has been derived from experimentally determined variations in the solubility of different silica species in water, as a function of temperature. The basic reaction for a solution of silica minerals to give dissolved silica is

$$Si\,O_2\,(s) + 2\,H_2\,O \Rightarrow H_4\,Si\,O_4\,(aq)$$

The solubility of quartz appears to control dissolved silica in geothermal reservoirs at temperatures higher than 120-180˚C. The silica (quartz) geothermometer, proposed by Fournier and Rowe (1966), could be used in the range 120-330˚C, with the following assumptions: the fluid is in equilibrium with quartz in the reservoir, the pore-fluid pressure in the reservoir is fixed by the vapour pressure of pure water, there is no mixing of hotter and colder waters during upflow, and there is neither conductive cooling of the ascending water nor adiabatic cooling with steam separation at 100˚C.

Fournier (1973) presented the quartz geothermometer with maximum steam loss at 100˚C as a function of the silica concentration (SiO_2 is in mg/kg):

$$t(^{\circ}C) = \frac{1522}{5.75 - \log SiO_2} - 273.15 \qquad (14)$$

The most widely used formula for the quartz geothermometer (Fournier and Potter, 1982) and the one used in this study is

$$t(^{\circ}C) = -42.198 + 2.883\times10^{-1}S - 3.668\times10^{-4}S^2 + 3.1665\times10^{-7}S^3 + 70.34\log S \qquad (15)$$

3.2.3 Chalcedony geothermometer

This geothermometer is based on the solubility of chalcedony. Fournier (1991) pointed out that there is an ambiguity in the use of silica geothermometers at temperatures below 180˚C as chalcedony appears to control dissolved silica in some places and quartz in others. Chalcedony is a very fine-grained variety of quartz, which is probably not a separate mineral but a mixture of quartz and moganite (Gíslason et al., 1997) and with time it probably all changes to quartz. Temperature, time and fluid composition all affect different crystalline forms of silica. Thus, in some places (old systems), where water has been in contact with rock at a given temperature for a relative long time, quartz may control dissolved silica at temperatures down to 100˚C. In other places (young systems), chalcedony may control dissolved silica at temperatures up to 180˚C.

The chalcedony geothermometer at the condition of maximum steam loss presented by Arnórsson et al. (1983b) is:

$$t(^{\circ}C) = \frac{1264}{5.31 - \log SiO_2} - 273.15 \qquad (16)$$

and without steam loss

$$t(^{\circ}C) = \frac{1112}{4.91 - \log SiO_2} - 273.15 \qquad (17)$$

Table 3 shows the results of the applications of the different geothermometers discussed above to the Berlín geothermal waters.

TABLE 3: Results of temperatures (˚C) using geothermometers

Sample	T_{NaK} (1)	T_{NaK} (2)	T_{NaK} (3)	T_{NaK} (4)	T_{KMg} (5)	T_{NaKCa} (6)	T_{quartz} (7)
TR-2	301	309	300	300	366	338	261
TR-4A	296	304	292	292	271	333	256
TR-4B	296	305	293	293	285	334	256
TR-4C	295	304	291	291	303	332	258
TR-5A	274	285	263	265	179	315	248
TR-9	287	297	281	282	367	326	245

(1) Fournier (1979) (2,5) Giggenbach (1988) (3) Truesdell (1976)
(4,8) Arnórsson et al. (1983b) (6) Fournier and Truesdell (1973) (7) Fournier and Potter (1982)

3.2.4 Solution-mineral equilibria

The application of various geothermometers to the same field frequently yields different values for reservoir temperature. Reed and Spycher (1984) proposed the calculation of multicomponent fluid-mineral equlibria in geothermal systems, and its application to geothermometry. They pointed out that if a group of minerals approaches equilibrium at a particular temperature, this temperature corresponds to the most likely reservoir temperature, or at least the source aquifer temperature of the particular water considered. For the dissolution of a mineral *m*, the saturation index log (Q_m/K_m) can be written as the following equation:

$$\log(Q_m/K_m) = \log[(\Pi a_{i,m}^{v_{i,m}})/a_m/K_m] \qquad (18)$$

where $a_{i,m}$ is the activity and $v_{i,m}$ is the stoichiometric coefficient of species i for mineral m. The reaction equation is written with the mineral on the left hand side, and the aqueous components on the right hand side, the activity of mineral m, a_m, being equal to one for pure minerals; K_m is the equilibrium constant for mineral m at a specific temperature.

The calculation, can be performed using the WATCH computer program of Arnórsson et al. (1983a) and Bjarnason (1994) to construct the mineral equilibria diagram of minerals for deep water corresponding to the samples, shows the saturation index, ionic balance, geothermometer (quartz, chalcedony and Na/K) values and log (Q/K).

a) The ionic balance is a good tool for checking the analytical results. The value is close to zero if the analyses are accurate and high if the analytical results are not accurate. For dilute waters, values in the range ± 10% are considered acceptable.
b) The deep water temperatures were calculated with the use of various geothermometers (quartz, chalcedony, and Na/K). The quartz temperature was used as a reference temperature when the speciation of the waters was calculated. As the Berlín geothermal field is a high-temperature field, the use of quartz temperature as a reference temperature is assumed to give the most reliable results. Nevertheless, quartz often gives slightly low temperature values at high temperatures (>250˚C) and Na/K may be closer to the correct reservoir value, because it does not re-equilibrate so fast to give a new value, and this is confirmed if account is taken of the measured reservoir temperature (295-300˚C).
c) The log solubility product of minerals was calculated for the geothermal samples collected in the period mentioned earlier. The speciation of the fluids sampled was calculated using the WATCH program in the temperature range 100-350˚C.

4. MIXING MODELS

Water formed by the mixing of geothermal water with cold ground or surface water possesses many chemical characteristics which serve to distinguish it from unmixed geothermal water. The reason is that the chemistry of geothermal water is characterised by equilibrium conditions between solutes and alteration minerals at relatively high temperatures, whereas the composition of cold water appears to be mostly determined by the kinetics of the leaching process (Arnórsson, 1985).

Ascending hot water may take diverse routes to the surface. Geothermal water which ascends from a reservoir and emerges at the surface in hot springs, may cool by conduction, boiling, mixing with colder water, or a combination of these processes. In addition, complete or partial chemical re-equilibration may occur as temperature decreases.

4.1 Schoeller diagram

The Schoeller diagram (Truesdell, 1991) compares the log concentration of fluid constituents from a number of analyses, with constituents of each analysis connected with a line. A wide range of concentrations can be shown, because logarithmic values are used. The effect of mixing with dilute water (as well as gain or loss of steam) is to move the line representing an analysis vertically without changing its shape. Slopes of lines between constituents represent concentration ratios. These diagrams show the effect of mixing on a number of constituents. When many analyses are shown, individual patterns may be lost, but the patterns of mixing will remain clear.

For presentation of water chemistry of the Berlin geothermal area, the most important constituents of the samples were plotted in such a diagram (Figure 8), where the log concentration of each constituent in each

sample is connected to another with a line.

The thermal water (solid lines) concentrations are, in general, higher in all constituents, particularly Li, Na, K, Cl and B. It can also be seen that the cold waters have a high concentration of Mg but the thermal waters are particularly low in this element. Also the cold water lines intersect the thermal water line suggesting that the thermal water of the Berlín area in particular is mixed with some cold water. This diagram is effective in showing this mixing and serves as an indicator of the water chemistry of the area.

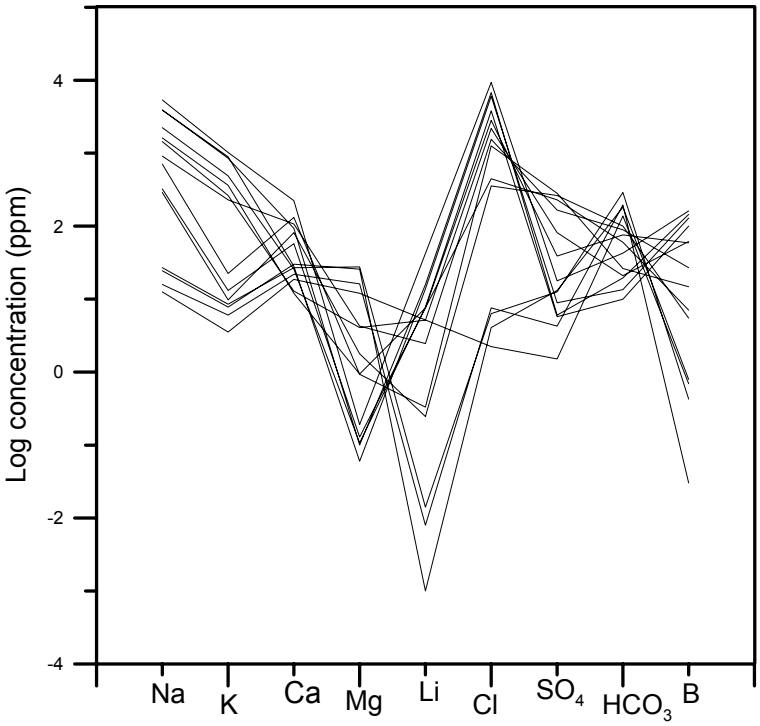

FIGURE 8: Schoeller diagram for the most important constituents in the Berlin waters

4.2 Silica-enthalpy mixing model

The water in many hot springs consists of mixtures of deep hot water and shallow cold water. Truesdell and Fournier (1977) have proposed a plot of dissolved silica versus enthalpy of water to estimate the temperature of the deep hot water component. This model is based on the assumption that no conductive cooling has occurred after mixing. If the mixed water has cooled conductively after mixing, the calculated temperature of the hot water component is too high. It is also assumed that no silica deposition takes place before or after mixing and that quartz controls the solubility of silica in hot water.

4.3 Enthalpy-chloride mixing model

Enthalpy-chloride diagrams have been used to predict underground temperatures, salinity, boiling and mixing relationships. Fournier (1977) suggested the use of an enthalpy-chloride diagram to predict underground temperature. This mixing model takes into account both mixing and boiling processes. Its application basically involves relating analysed chloride levels to water enthalpy, which can be derived from measured discharge temperature, geothermometry temperature and silica-enthalpy mixing model temperature.

4.4 Silica-carbonate mixing model

Arnórsson et al. (1983b) found that the concentrations of carbon dioxide in water in geothermal reservoirs were only dependent on the temperature of these waters. At temperatures above about 200˚C, most of the dissolved total carbonate is in the form of carbon dioxide, so it is a satisfactory approximation to take analysed carbonate to represent carbon dioxide. The silica levels in high-temperature waters are determined by quartz solubility, so it is a satisfactory approximation to assume a fixed relation between silica and total carbonate in high-temperature geothermal reservoir waters. Boiling of such water will lead to a drastic reduction in its carbonate content but mixing without boiling will, on the other hand, produce water with high carbonate/silica ratios relative to equilibrated water.

The silica-carbonate diagram may be used to aid geothermometry interpretation. First, it serves to distinguish boiled water from conductively cooled water and mixed water which contains an undegassed

hot water component, assuming that the boiling occurs between the points of last equilibrium with quartz and sampling. Secondly, if there is sufficient data on warm water containing an unboiled water component, it is possible to evaluate the temperature of the hot water component with the diagram.

Estimation of underground temperatures using the silica-carbonate mixing model involves extrapolation of a line through the data points for mixed and undegassed warm water and determination of the point of intersection with the silica-carbonate curve for equilibrated water. The quartz geothermometer is used to obtain the temperature from the silica concentration corresponding to this point.

5. GAS CHEMISTRY

5.1 Introduction

The percentage of total gas in geothermal steam (Tables 4 and 5), both in fumaroles and drillholes, varies greatly between fields as do the relative abundances of the most abundant gases (CO_2, H_2S, H_2, CH_4 and N_2). In geothermal reservoirs above 150-200˚C, equilibrium between CO_2, H_2S and H_2 and specific alteration minerals is generally closely approached. However, different minerals can be involved in different reservoirs.

TABLE 4: Gas composition of Berlín wells (in mmoles/100 moles; data from CEL)

Well	Date	H_2	Ar	N_2	CH_4	CO	H_2S	CO_2	NH_3	Total
TR-2	1995	1.23		3.92	0.32		8.58	168.73	0.12	182.89
TR-2	1996	1.95		2.49	0.28		11.19	122.19	0.08	138.18
TR-2	1997	1.33		2.49	0.30		11.16	117.46	0.08	132.81
TR-2	1997	1.22		2.74	0.29		12.46	126.58	0.13	143.41
TR-2	1998	1.46		1.20	0.29	0.01	16.42	113.53	0.17	133.17
TR-2	1998	1.83	0.13	2.64	0.24	0.09	13.63	125.60	0.01	144.17
TR-4B	1999	2.14	2.27	20.1	0.40	0.15	11.87	214.65	0.13	251.73
TR-4C	1998	12.8	46.2	42.8	1.80	0.69	29.73	976.91	0.08	1110.95
TR-4C	1999	1.83	2.27	20.9	0.40	0.16	15.06	274.48	0.09	315.24
TR-5	1995	1.15		0.62	0.27		13.05	70.10	0.08	85.27
TR-5	1996	1.69		3.12	0.29		14.91	100.12	0.10	120.23
TR-9	1995	1.50		2.95	0.31		13.57	178.47	0.14	196.94
TR-9	1996	1.61		2.65	0.32		13.34	125.45	0.01	143.38
TR-9	1997	1.82		3.55	0.34		12.32	184.41	0.15	202.59
TR-9	1998	1.93	0.14	1.61	0.27	0.10	16.24	194.09	0.08	214.46
TR-9	1998	1.79	0.13	2.77	0.24	0.09	14.87	214.50	0.01	234.40

Gas chemistry of fumaroles has been used to predict subsurface temperatures, locate upflow zones and map the flow direction of boiling water underground. Gas composition of well discharges has been used to evaluate the temperature of producing aquifers and the initial steam-to-water ratio in the reservoir, and boiling processes in the aquifer around producing wet-steam wells, including the extent of segregation of the flowing water and steam and heat flow from the rock, which enhances evaporation.

Generally, over 99% of the total gas in geothermal steam is composed of CO_2, H_2S, H_2, CH_4 (and other hydrocarbons), Ar, N_2 and NH_3. These gases are reactive chemically; they react with the rock, between themselves or with aqueous solutes. He, Ne and CO occur in trace amounts in geothermal steam.

The total gas concentration in geothermal steam varies immensely, from much less than 0.1% to over 10% by volume. Often there is a positive correlation between the concentrations of some gas components, like CO_2, H_2S, and H_2, within geothermal fields. Carbon dioxide is usually the major gas component.

TABLE 5: Gas composition of fumarole steam in the Berlín geothermal area (in mmoles/100 moles)

Fumarole	H_2	N_2	Ar	CH_4	H_2S	CO_2	NH_3	$\delta^{18}O$ (‰)	$\delta^{2}H$ (‰)	Temp. (˚C)
Tronador	2.9	5.03		0.31	3.71	246.5	0,09	-5.05	-44.58	99
Tronadorcito	2	62.3		0.30	7.09	2531	0.33	-8.33	-54.52	97
El Zapote	1.3	4.78		0.28	4.96	252.4	0.175			98
El Zapotillo	0.9	5.56		0.25	4.15	274.1		-8.09	-53.60	
El Bálsamo	1.7	3.57		0.31	5.35	236.9	0.42	-13.5	-81,28	99
La Joyona	88	1458	2.25	6.22	37.8	83608	0.08			98
El Hoyón	58	20.4	0.16		199	3078	0.01	-11.8	-79.56	98
Lag. Alegría	6.7	130	1.04	1.30	2823	7058	0.01			97
Trujillo	2	10.2	0.14	0.32	4.27	291.5	0.32	-11.7	-73.15	98
Calaboz	47	1059	1.71	0.61	382	43973	0.05			98
Grieta TR-6	2.6	3.72		0.31	5.21	244	0.36	-6.68	-46.63	98

5.2 Gas geothermometers and equilibria associated with gases

In almost all geothermal fields, surface manifestations consist of fumaroles, steam heated waters, and hot altered ground. Since the 1970's, studies have successfully demonstrated that gas components from fumarole and well discharges can be used as geothermometers (e.g. Tonani, 1973; Arnórsson and Gunnlaugsson, 1985; D'Amore and Panichi, 1980; D'Amore, 1991; Giggenbach, 1991).

The temperature equations for the gas geothermometers presented below are considered to correspond to equlibria between the respective gases and specific mineral buffers. Calcite, together with quartz, epidote and prehnite above about 230˚C, and various zeolites in addition to calcite may possibly be involved at lower temperatures (Arnórsson and Gunnlaugsson, 1985). Iron minerals and iron-containing aluminium silicates such as pyrite + pyrrhotite + epidote + prehnite, magnetite + epidote + prehnite and/or pyrite + epidote + prehnite + chloride may constitute the H_2S and H_2 buffers (Giggenbach, 1980; Arnórsson and Gunnlaugsson, 1985).

The H_2 concentration is apparently controlled by the Fe-bearing minerals epidote and prehnite, which are also active in controlling the H_2S concentration and, thus, the H_2S/H_2 ratio. The dependence of this ratio on temperature can be shown easily but the geothermometer based directly on it does not work very well because of dissociation and redox reactions of H_2S.

In this report, the five gas geothermometers from Arnórsson and Gunnlaugsson (1985) were applied to fumarole steam and steam from wet steam wells in the Berlín high-temperature geothermal field as follows (concentration in mmoles/kg steam):

CO_2 geothermometer, temperature range 100-330˚C:

$$T_{CO_2} = -44.1 + 269.25 \log m_{CO_2} - 76.88 (\log m_{CO_2})^2 + 9.52 (\log m_{CO_2})^3 \quad (19)$$

H_2S geothermometer, in the temperature range 200-300˚C with C1 < 500 ppm:

$$T_{H_2S} = 173.2 + 65.04 \log m_{H_2S} \quad (20)$$

H_2 geothermometer, in the temperature range 200-300˚C with C1 < 500 ppm:

$$T_{H_2} = 212.1 + 38.59 \log m_{H_2} \quad (21)$$

CO_2/H_2 geothermometer, in the temperature range 200-300˚C with C1 < 500 ppm:

$$T_{CO_2/H_2} = 311.7 - 66.72\log(m_{CO_2}/m_{H_2}) \quad (22)$$

CO_2/N_2 geothermometer (Arnórsson, 1987)

$$T(^{\circ}C) = 148.5 + 64.35\log(m_{CO_2}/m_{n_2}) + 5.239[\log(m_{CO_2}/m_{n_2}]^2 - 1.832[\log(m_{CO_2}/m_{n_2}]^3 \quad (23)$$

Geothermal gases are originally introduced into the geothermal fluid with recharge water from water rock interaction in the reservoir or from a magmatic fluid invasion. In an undisturbed reservoir, reactions at equilibrium at the reservoir temperature control the concentrations of these gases.

Table 6 shows the results for temperatures of the well and fumarole reservoir fluids using the different geothermometers mentioned above.

TABLE 6: Results of gas geothermometers (˚C) for fumarole and wet-steam well fluids in the Berlín area

Sample	T_{CO2}	T_{H2S}	T_{H2}	$T_{CO2/H2}$	$T_{CO2/N2}$
TR-2/95	261	217	206	169	211
TR-2/96	250	224	213	192	213
TR-2/97	248	224	207	182	212
TR-2/97	251	227	206	177	212
TR-2/98	246	235	209	181	213
TR-2/98	251	230	212	189	212
TR-2/99	266	257	263	191	209
TR-4B/98	269	226	215	178	187
TR-4B/99	271	232	214	173	193
TR-4C/98	276	233	212	166	190
TR-4C/99	273	234	211	167	195
TR-5/95	228	228	205	193	225
TR-5/96	242	232	211	193	206
TR-9/95	263	229	209	173	216
TR-9/96	251	229	210	185	212
TR-9/97	264	228	212	178	214
TR-9/98	266	234	213	178	226
TR-9/98	269	323	212	173	220
TR-9/99	266	242	220	189	217
Tronador	273	193	218	180	213
Tronadorcito	339	211	214	105	210
El Zapotillo	276	196	201	147	213
El Bálsamo	272	203	211	169	217
La Joyona	506	258	277	113	215
El Hoyón	345	304	270	197	229
Lag. Alegría	372	314	234	110	214
Trujillo	278	197	214	168	204
Calaboz	461	322	267	113	210
Grieta TR-6	273	203	218	180	217

6. RESULTS

6.1 Type of water and possible origin

Isotopic composition of water. The local meteoric water line is obtained for the rainy season. Probably this is evaporated water that is assumed to be percolated into the ground (all samples collected in the summer season show intense evaporation and are not considered in the correlation). It is defined by the equation:

$$\delta^2 H = 7.92\,\delta^{18}O + 9.51 \qquad (24)$$

with a correlation of 0.992. It is possible to see that the equation is almost the same as that for the World Meteoric Line; the difference being due to the climatic conditions in the area.

Figure 4 shows the isotopic composition of deep geothermal water, cold and hot spring water, and reinjection water. Comparing isotope data on rainwater from different altitudes and locations, with those on on the thermal water it is possible to infer origin of the recharge of Berlín geothermal field and the value obtained for the altitude was 1350 m a.s.l.; this value is in agreement with the results of hydrologic and geologic studies (Correia et al., 1996). The upflow area is probably located in the fumarole zone for the old wells (TR-2 and TR-9). It could be El Hoyón (in agreement with studies carried out by CEL). For the other wells, it could be Tronadorcito or/and El Zapotillo.

The Cl-SO_4-HCO_3 triangular diagram. In order to classify water, the relative concentrations of the main anions of the spring water (hot and cold) and well water from the Berlín geothermal area, are plotted in Figure 5. The figure shows that most of the spring water plots in the bicarbonate corner, with the exception of eight hot springs whose chloride content is anomalous. This is typical for water associated with high-temperature systems, probably of volcanic origin, but considerably diluted due to mixing with meteoric water (Figure 5) during its rise to the surface as was mentioned earlier. These are characterised by high total dissolved solids, chloride concentration and temperatures between 64 and 98˚C. Samples plotting near the chloride corner are located in the northeastern part of the well field near Lempa River.

Most chloride waters are discharged from geothermal wells. High chloride, but low sulphate and bicarbonate water is typical for high-temperature systems associated with andesitic and rhyolitic magmatism.

Cl-Li-B triangular diagram. A plot of the relative concentrations of chloride, boron and lithium is shown in Figure 6. Mass ratios like the Cl:B, Na:K and Na:Li suggest homogenous fluid source at depth. The geothermal well water and most of the spring water at Berlín plot near the Cl-B tie line. Relative Cl and B contents suggest either the addition of these two elements before, during or after the rock dissolution process, or loss of Li.

The distribution data points of the geothermal system with close volcanic magmatic associations, may be explained in terms of the dissolution of rock in water formed through the absorption of high-temperature, high-pressure, magmatic vapour in deeply circulating groundwater. These vapours may contain Cl and B in proportions close to those of the crustal rocks contacted. The boron content of thermal fluids is also likely to reflect, to some degree, the maturity of a geothermal system. Because of its volatility it is likely to be expelled during the early heating-up stages. Therefore, fluids from "older" hydrothermal systems can be expected to be depleted in B. Data points close to the Cl corner may represent water formed through the absorption of, in this case, low B/Cl magmatic vapour.

6.2 Estimation of subsurface temperature

In order to identify the equilibrium status of the geothermal fluids, a Na-K-Mg triangular diagram (Giggenbach, 1988) was drawn (Figure 7). The points in the figure fall mainly into three groups.

a) Immature water, all cold springs and the hot spring F-144 plot in this region.
b) Equilibrated water, well discharges plot, as expected, close the full equilibrium line at their deep temperature and this is between 280 and 320˚C in the figure. Exceptions are the new wells (TR-4B and TR-4C) drilled in 1998 and they still contain drilling fluid. But some of the data from wells plot beyond the theoretical lines due to steam loss increasing absolute solute contents of these samples collected at atmospheric pressure.
c) Mixed and boiled/degassed waters, i.e. the hot springs F-126, F-128, F-129, F-145, F-144B and F-20.

Clearly, the use of cation geothermometers for most well discharges in the field is justified. The results for different geothermometers are shown in Table 3. All the samples lie in the temperature range 247-264˚C for quartz, 236-255˚C for chalcedony, 274-301˚C for Na/K (Fournier, 1979), 265-300˚C for Na/K (Arnórsson et al., 1983b), 285-309˚C for Na/K (Giggenbach, 1988), 263-300˚C for Na/K (Truesdell, 1976). For the Na-K-Ca temperature (Fournier and Truesdell, 1973), all samples lie in the range of 315-338˚C, and 179-367˚C for K/Mg. All Na-K geothermometry equations give a good match with measured aquifer temperature (270-300˚C). The Na-K-Ca geothermometer indicates higher temperature and so does the K-Mg geothermometer. The quartz and chalcedony geothermometers indicate lower temperatures, part of the difference probably due to the loss of these minerals during the ascension of water.

As discussed in Section 5.1, the concentrations of various gases in fumarole steam and steam from wet-steam wells are considered to be in equilibrium with mineral buffers at any given temperature. Five gas geothermometers were used for this report. Results are presented in Table 6. For wells and fumaroles, the CO_2 geothermometer gives the highest temperature values an average of 286˚C, which agrees with the measured temperature (280-305˚C). The H_2S geothermometer indicates aquifer temperature of 237˚C. The H_2 geothermometer gives an average subsurface temperature of 220˚C. The CO_2/H_2 geothermometer gives the lowest subsurface temperature values of 169˚C. The CO_2/N_2 geothermometers give a temperature of 211˚C.

The discrepancy between the estimated subsurface temperatures obtained by various gas geothermometers may be explained by various causes. One is that it is a relatively old geothermal system which means that the geothermal system has cooled down, and such a system tends to be high in CO_2 and yield high CO_2 geothermometer temperatures. For the high CO_2 concentration in such systems, various explanations have been offered, one being that there is probably a steady flow of CO_2 from the magma which becomes masked in the high concentration in new systems but with lowered equilibrium concentrations along with a reduced steam fraction. As speculated by Arnórsson and Gunnlaugsson (1985) and Zhao Ping and Ármannsson (1996), different mineral buffers may control H_2S and H_2 concentrations at different temperatures. The low H_2S temperatures are due to loss of H_2S by oxidation, especially for the samples collected on high ground.

6.3 Application of the computer program WATCH

The results of chemical analysis of samples from the Berlín geothermal field were evaluated, using the computer programs WATCH and SOLVEQ. The WATCH program (water chemistry version 2.1) is an updated unified version of WATCH1 and WATCH 3 (Arnórsson et al., 1982) revised by Bjarnason (1994). The new version uses the same thermodynamic data. WATCH reads chemical analysis of water, gas and steam samples, and computes aqueous speciation, gas pressure, and activity and solubility products at the designated temperature. It also allows the equilibrated fluid to be cooled conductively or adiabatically from the reference temperature to a lower temperature. The input file for WATCH can be created by the program WAIN (Bjarnason, 1994).

Figure 9 represents a log (Q/K) (saturation index) versus temperature diagram for anhydrite, calcite,

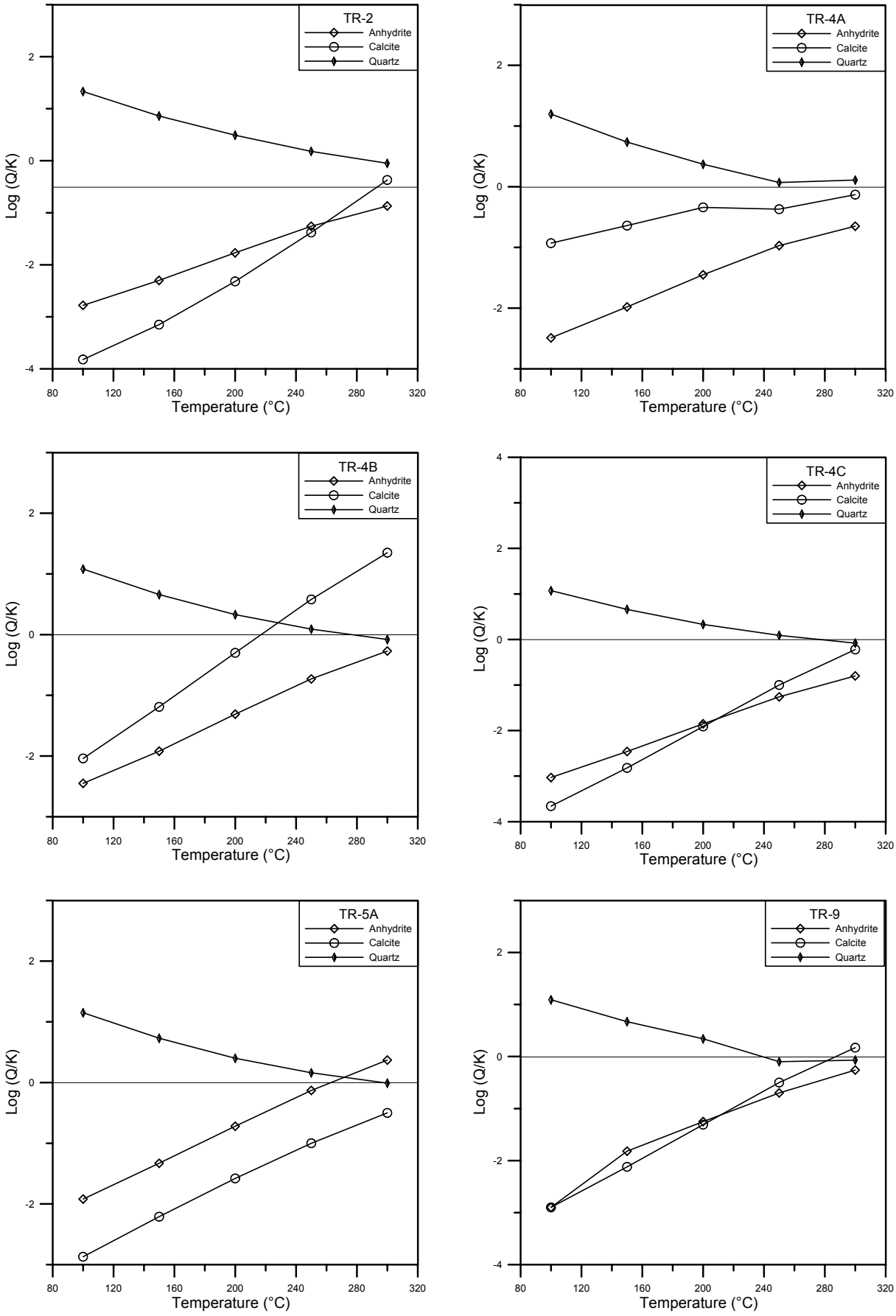

FIGURE 9: Saturation index (log Q/K) vs. temperature for anhydrite, calcite and quartz for adiabatic boiling of Berlín wells

amorphous silica, chalcedony and quartz for adiabatic boiling of Berlín wells, calculated with the aid of WATCH program. For all wells, the water is close to equilibrium with quartz, chalcedony and amorphous silica and undersaturated with calcite and anhydrite. According to the diagrams from the Berlín wells in the figure, boiling leads to sharp supersaturation with respect to quartz, and also supersaturation with respect to amorphous silica and chalcedony around 100˚C.

Nevertheless, in the diagrams no best equilibrium temperatures can be found, probably owing to mixing, degassing/boiling and other relevant processes such as the precipitation of some minerals. But, in general in the reservoir, temperature seems to fall between 240 and 300˚C. As Al analyses were not available, only very few minerals were considered.

According to the results obtained by the WATCH program, the potential for silica scaling in the Berlín fluids is still high as is indicated in Figure 9 and the maximum degree of supersaturation occurs between 100 and 240˚C.

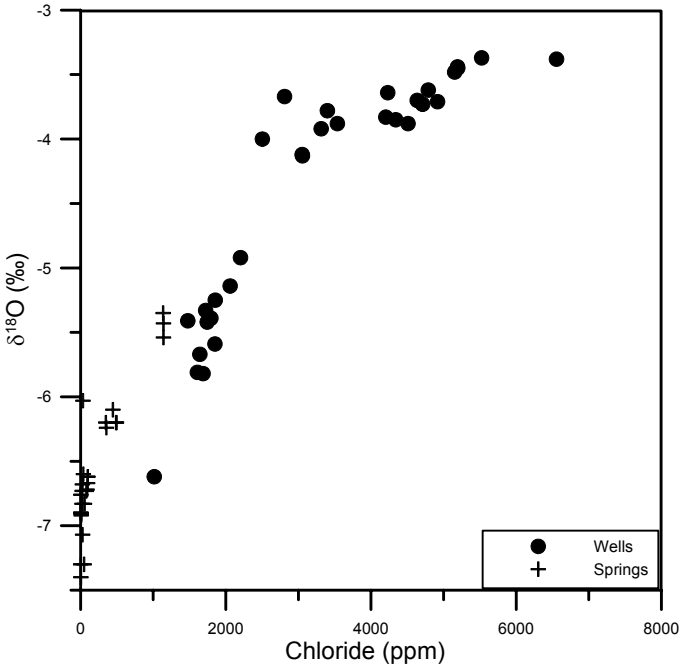

FIGURE 10: $\delta^{18}O$ vs. Cl for Berlín waters

6.4 Evaluation of mixing processes

Evidence of mixing. As mentioned, there is some evidence that ascending hot water has mixed with cold water. The evidence is the following:

a) Linear relationship between $\delta^{18}O$ and chloride (Figure 10). This relationship is thought to constitute particularly valuable evidence of mixing (Arnórsson, 1985).
b) Linear relationship between chloride and boron and a positive relationship between chloride and sodium; Figure 11 shows plots for both. Unfortunately, the chloride concentration of precipitation in the area is unknown.
c) On the Na-K-Mg triangular diagram (Figure 7), some thermal samples fall in the area of mixed or partially equilibrated waters.

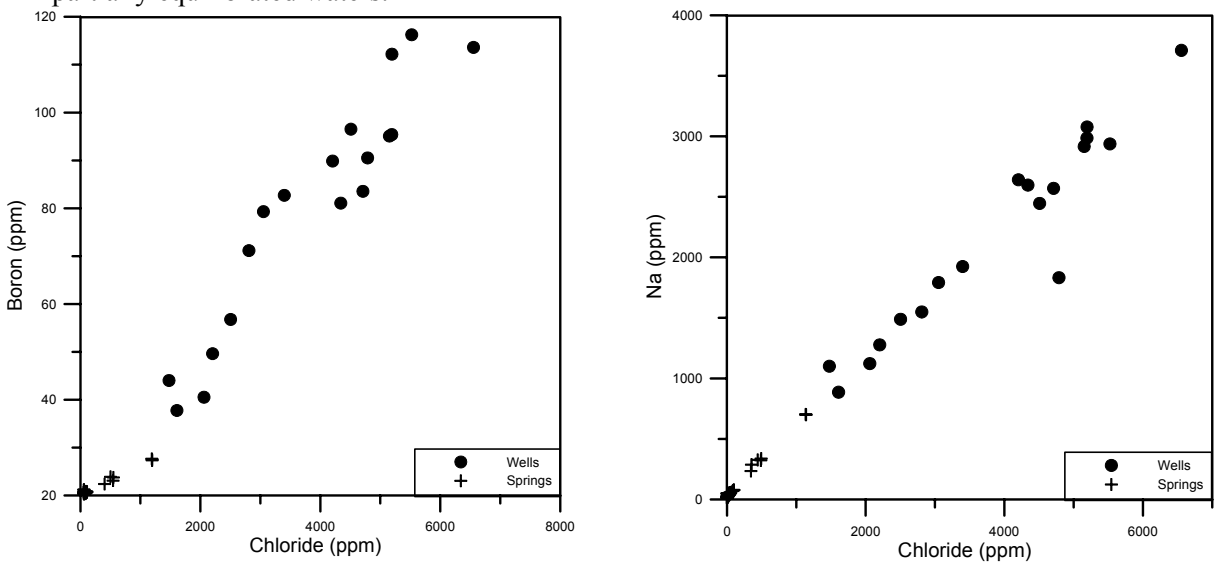

FIGURE 11: Chloride vs. boron and sodium for the Berlín waters

Three mixing models were applied to the water in this study, the silica-enthalpy mixing model (Fournier, 1981), silica-carbonate mixing model (Arnórsson, 1985), and the chloride-enthalpy mixing model (Truesdell and Fournier, 1977).

The enthalpy-chloride-mixing model. Diagram plots are simple but have proved very useful in determining models of fluid movements and hydrology by considering chloride concentration and enthalpy. It is possible to use these diagrams in both exploration and development stages and they are successful for virtually all types of terrain and for both high and low temperature.

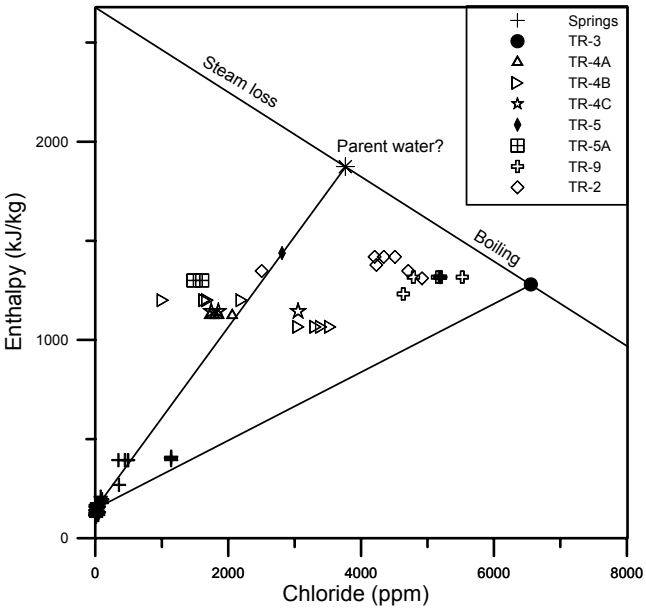

FIGURE 12: Enthalpy-chloride mixing model for the Berlín wells and spring waters from the northern part of the field

This mixing model takes into account both mixing and boiling processes. The results for the Berlín geothermal water and spring water from the northern part of the field are shown in Figure 12. It is clear that two types of water are observed, surface and thermal water. Well TR-3 has been subjected to boiling processes, and steam loss produces loss of heat and increase in chloride content in the liquid phase (through loss of mass, i.e. vapour). On the other hand, most of the geothermal well water plots in the mixing zone and also some of the well water have been subjected to a certain degree of mixing and boiling. Some of them (TR-4B and TR-4C) plot outside the mixing zone but probably they reach the mixing zone after stabilisation. Well TR-5A water could be dilute water (little increase in Cl) that has taken up heat.

It is also observed that wells TR-2 and TR-9 are different. TR-2 could be subject to dilution with meteoric water since the well water is depleted in heavy isotopes, and in TR-9 some boiling may have occurred as there is a general enrichment in isotopes and chloride. These results are in agreement with the results presented in Figure 13, the isotope ($\delta^{18}O$ and $\delta^{2}H$) vs. chloride diagrams.

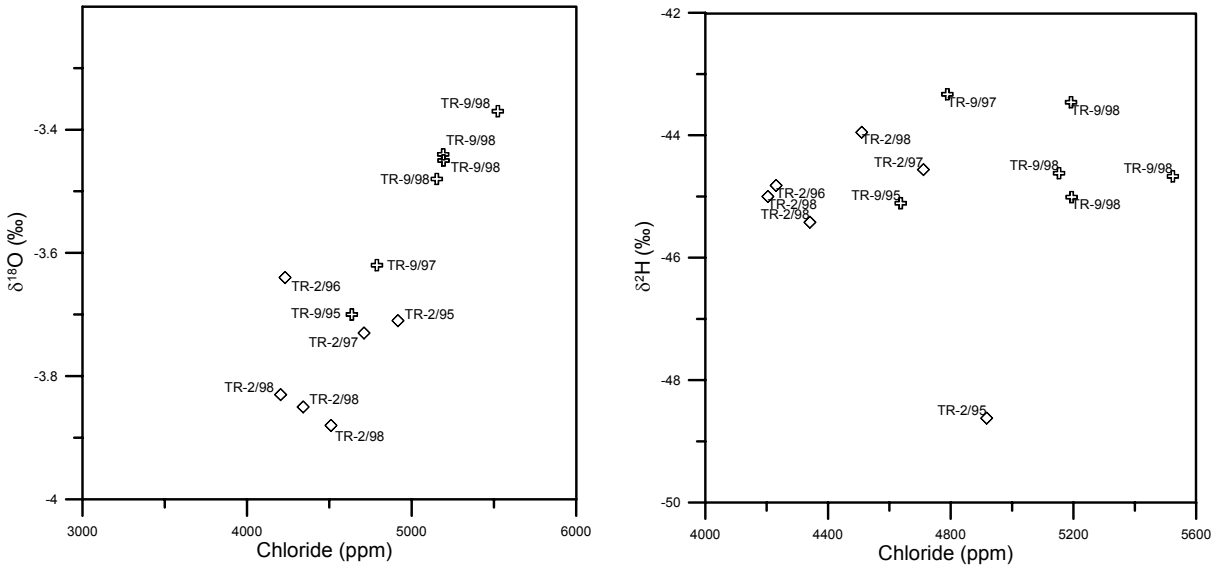

FIGURE 13: The relationship between chloride and heavy isotopes for Berlín well waters

The silica-enthalpy mixing model. As was discussed earlier, silica vs. enthalpy of the liquid water is used to estimate the temperature of the mixed water. Enthalpy is used as a co-ordinate rather than temperature. This is because the combined heat contents of two waters at different temperatures are conserved when those waters are mixing, but the combined temperatures are not.

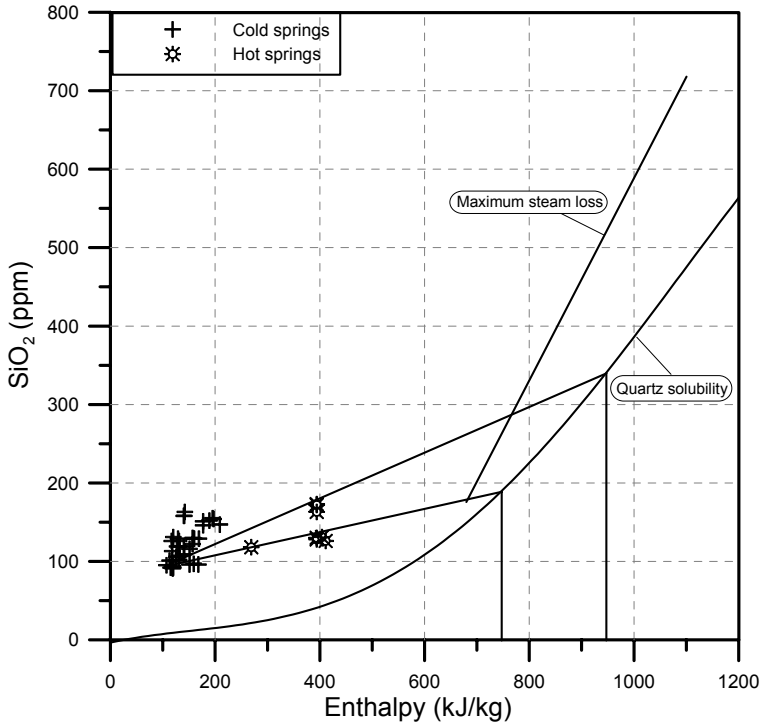

FIGURE 14: Silica-enthalpy mixing model for the Berlín waters

Figure 14 depicts the silica-enthalpy-mixing model applied to the Berlín data. For these data two mixing lines result. Assuming no steam loss before mixing, both lines are drawn from the cold water samples through the hot springs. The estimated enthalpies for the deep hot water are 740 and 920 kJ/kg, which correspond to temperatures of 174 and 216˚C, respectively.

The silica-carbonate mixing model. Figure 15 depicts the silica-carbonate-mixing model. The hot spring values fall on the SiO_2-CO_2 curve, suggesting no mixing.

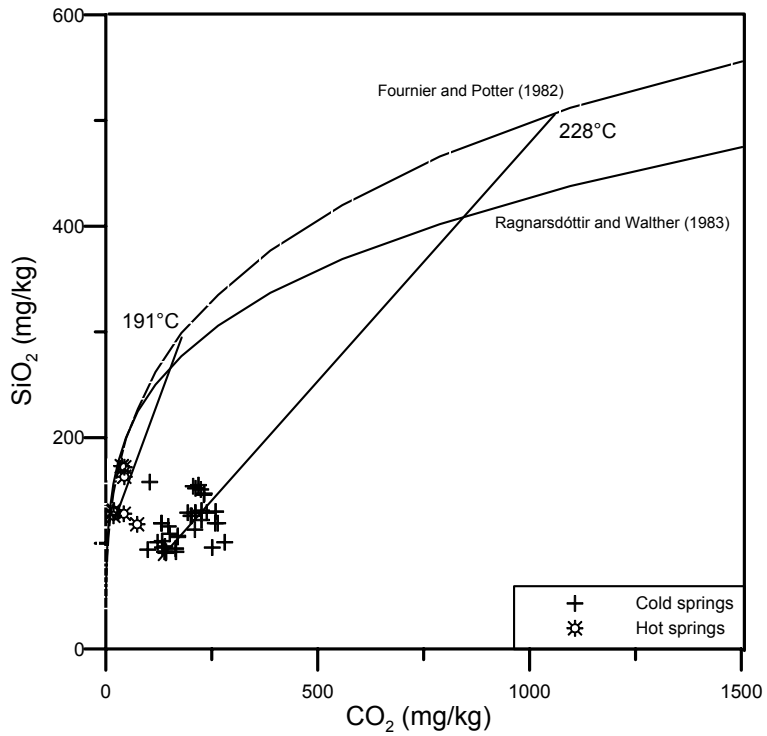

FIGURE 15: Silica-carbonate mixing model for the Berlín waters

7. CONCLUSIONS

The main objectives of this project were to study the chemical characteristics of thermal fluids from the Berlín geothermal field, to define mixing and the main origin of mixed water, and to study and predict the subsurface temperature. The conclusions are as follows:

1. The geothermal water of Berlín field is Na-Cl type but the cold springs are of the Na-HCO_3 type. The hot springs plot in the Cl part, and minor changes can be detected in the chemical and isotopic composition of the discharging fluids from wells TR-2 and TR-9 between 1995 and 1998.
2. There is evidence of mixing between hot and cold water in the hot springs. Linear relationships between chloride, boron and sodium constitute the main evidence for mixing. The relationship between chloride and silica is not good due to silica-dependent temperature.
3. The mixing models applied to water in the study area, suggest a reservoir temperature ranging between 174 and 228˚C.
4. The thermal fluid is recharged by cold groundwater. The recharge zone is in Tecapa hill according to isotopic results and is in agreement with hydrologic and geologic studies. The upflow area is probably located close to some fumaroles: El Hoyón, Tronadorcito and El Zapotillo.
5. The stable isotope $\delta^{18}O$ and $\delta^{2}H$ relationship suggests that the source of the thermal fluid is a mixture of andesitic water (Giggenbach, 1992) and meteoric water. They produce an oxygen shift due to andesitic water or water-rock interaction at low permeability.
6. The depletion and enrichment in heavy isotopes observed in wells in Berlín area is probably due to dilution and boiling processes.
7. The boiled water from Berlín wells is supersaturated with respect to amorphous silica, chalcedony and quartz. The SI for quartz (saturation index) vs. temperature is quite close to equilibrium.

ACKNOWLEDGEMENTS

I would like to express my heartfelt gratitude to Dr. Ingvar Birgir Fridleifsson and Mr. Lúdvík S. Georgsson for giving me the opportunity to attend the UNU Geothermal Programme, and for their moral support and help throughout the whole training period. I am much obliged to Dr. Halldór Ármannsson, my advisor, for his help and critical advice during the preparation of this report. I wish to give thanks to all the lecturers, especially to Dr. Stefán Arnórsson for his excellent thermodynamic lectures, and to the staff members at Orkustofnun for their comprehensive presentations and willingness to share their knowledge and experience. Mrs. Gudrún Bjarnadóttir deserves my thanks for daily arrangements and help during the course.

I also express my gratitude to the Comisión Ejecutiva Hidroeléctrica del Río Lempa (CEL), especially to the Gerencia de Recursos Geotérmicos for giving me the opportunity to participate in this programme and also for providing me with the necessary information used in this report.

Finally, I am deeply grateful to my family, for their spiritual support during these six months.

REFERENCES

Arnórsson, S., 1985: The use of mixing models and chemical geothermometers for estimating underground temperature in geothermal systems. *J. Volc. Geotherm. Res., 23,* 299-335.

Arnórsson, S., 1987: Gas chemistry of the Krísuvik geothermal field, Iceland, with special reference to evaluation of steam condensation in upflow zones. *Jökull, 37,* 31-47.

Arnórsson, S., and Gunnlaugsson, E., 1985: New gas geothermometers for geothermal exploration - calibration and application. *Geochim. Cosmochim. Acta, 49,* 1307-1325.

Arnórsson, S., Gunnlaugsson, E., and Svavarsson, H., 1983a: The chemistry of geothermal waters in Iceland II. Mineral equilibria and independent variables controlling water compositions. *Geochim. Cosmochim. Acta*, *47*, 547-566.

Arnórsson, S., Gunnlaugsson, E., and Svavarsson, H., 1983b: The chemistry of geothermal waters in Iceland III. Chemical geothermometry in geothermal investigations. *Geochim. Cosmochim. Acta, 47*, 567-577.

Arnórsson, S., Sigurdsson, S. and Svavarsson, H., 1982: The chemistry of geothermal waters in Iceland I. Calculation of aqueous speciation from 0˚C to 370˚C. *Geochim. Cosmochim. Acta, 46,* 1513-1532.

Bjarnason, J.Ö., 1994: *The speciation program WATCH, version 2.1.* Orkustofnun, Reykjavík, 7 pp.

Correia, H., Jacobo, H., Castellanos, F., Tenorio, J., Handal, S., and Santos, P., 1996: *Synthesis of geo-scientific information of conceptual model of Berlín geothermal field.* Report submitted to CEL, (in Spanish), 50 pp.

D'Amore, F., 1991: Gas geochemistry as a link between geothermal exploration and exploitation. In: D'Amore, F. (coordinator), *Application of geochemistry in geothermal reservoir development.* UNITAR/UNDP publication, Rome, 93-117.

D´Amore, F., and Panichi, C., 1980: Evaluation of deep temperatures in geothermal systems by a new gas geothermometer. *Geochim. Cosmochim. Acta, 44,* 549-556.

Fournier, R.O., 1973: Silica in thermal waters. Laboratory and field investigations. *Proceedings of the International Symposium on Hydrogeochemistry and Biochemistry, Tokyo, 1*, *Clark Co., Washington D.C.,* 122-139.

Fournier, R.O., 1977: Chemical geothermometers and mixing model for geothermal systems. *Geothermics, 5,* 41-50.

Fournier, R.O., 1979: A revised equation for the Na-K geothermometer. *Geoth. Res. Council Transactions, 3,* 221-224.

Fournier, R.O., 1981: Application of water chemistry to geothermal exploration and reservoir engineering. In: Rybach, L., and Muffler, L.J.P. (editors), *Geothermal systems: Principles and case histories*. John Wiley and Sons Ltd., Chichester, 109-143.

Fournier, R.O., 1991: Water geothermometers applied to geothermal energy. In: D'Amore, F. (coordinator), *Applications of Geochemistry in Geothermal Reservoir Development*. UNITAR/UNDP publication, Rome, 37-69.

Fournier, R.O., and Potter, R.W. II, 1979: Magnesium correction to the Na-K-Ca chemical geothermometer. *Geochim. Cosmocim. Acta, 43*, 1543-1550.

Fournier, R.O., and Potter, R.W. II, 1982: A revised and expanded silica (quartz) geothermometer. *Geoth. Res. Council Bull., 11-10*, 3-12.

Fournier, R.O., and Rowe, J.J., 1966: Estimation of underground temperatures from the silica contents of water from hot springs and wet steam wells. *Am. J. Sci., 264,* 685-697.

Fournier, R.O., and Truesdell, A.H., 1973: An empirical Na-K-Ca geothermometer for natural waters.

Geochim. Cosmochim. Acta, *37*, 1255-1275.

GENZL, 1995: *Development of complementary geo-scientific studies in Berlín geothermal field.* CEL, report of research contact No. 2301, 65 pp.

Giggenbach, W.F., 1980: Geothermal gas equilibria. *Geochim. Cosmochim. Acta, 44,* 2021-2032.

Giggenbach, W.F., 1988: Geothermal solute equilibria. Derivation of Na-K-Mg-Ca geoindicators. *Geochim. Cosmochim. Acta, 52,* 2749-2765.

Giggenbach, W.F., 1991: Chemical techniques in geothermal exploration. In: D'Amore, F. (coordinator), *Applications of geochemistry in geothermal reservoir development*. UNITAR/UNDP publication, Rome, 119-142.

Giggenbach, W.F., 1992: Isotope shift in waters from geothermal and volcanic systems along convergent plate boundaries and their origin. *Earth and Planetary Sci. Lett., 113*, 495-510.

Gíslason, S.R., Heaney, P.J., Oelkers, E.H. and Schott, J. 1997: Kinetic and thermodynamic properties of moganite, a novel silica polymorph. *Geochim. Cosmochim. Acta, 61,* 1193-1204.

Magaña, M. I., 1998: *Chemical study and isotopic evolution of Berlín geothermal field during 1995-1998.* IAEA, Vienna, report (in Spanish), 10 pp.

Matus, A., Guevara, W., Montalvo, F., and Magaña, M., 1999: Determination of recharge and evolutionary study in new wells at Berlín geothermal field, using isotopes. *International Symposium on Isotope Techniques in Water Resources, Development and Management, May 1999, Book of Extended Synopses, Vienna, Austria*.

Monterrosa, M., 1993: *A 3-D natural state modelling and reservoir assessment for the Berlín geothermal field in El Salvador, C.A*. UNU G.T.P., Iceland, report 11, 45 pp.

Ragnarsdóttir, K.V., and Walther, J.V., 1983: Pressure sensitive "silica geothermometer" determined from quartz solubility experiments at 250˚C. *Geochim. Cosmochim. Acta, 47,* 941-946.

Reed, M.H., and Spycher, N.F., 1984: Calculation of pH and mineral equilibria in hydrothermal water with application to geothermometry and studies of boiling and dilution. *Geochim. Cosmochim. Acta, 48*, 1479-1490.

Tonani, F., 1973: Equilibria that control the hydrogen content of geothermal gases. *Bull. Volcanol., 44,* 547-564.

Truesdell, A.H., 1976: Summary of section III - geochemical techniques in exploration. *Proceedings of the 2nd U.N. Symposium on the Development and Use of Geothermal Resources, San Francisco, 1,* liii-lxxix.

Truesdell, A. 1991: Effects of physical processes on geothermal fluids. In: D'Amore, F. (coordinator*), Applications of Geochemistry in Geothermal Reservoir Development*. UNITAR/UNDP publications, Rome, 71-92.

Truesdell, A.H., and Fournier, R.O., 1977: Procedure for estimating the temperature of a hot water component in a mixed water using a plot of dissolved silica vs. enthalpy. *U.S. Geol. Survey J. Res., 5,* 49-52.

Zhao Ping, and Ármannsson, H., 1996: Gas geothermometry in selected Icelandic geothermal fields with comparative examples from Kenya. *Geothermics, 25-3,* 307-347.